Int. J. Solids Structures, 1971, Vol. 7, pp. 193 to 211. Pergamon Press. Printed in Great Britain

MOTION OF A FINITE RIGID STRIP IN AN ELASTIC HALF-SPACE SUBJECTED TO BLAST WAVE LOADING†

STEPHEN A. THAU‡

Illinois Institute of Technology, Chicago, Illinois

Abstract—An elastic half-space in which a thin rigid-smooth strip of length l is embedded just below and perpendicular to the surface is considered. The strip is subjected to planar, incident, compressional and shear waves which are generated by a steadily moving pressure wave on the surface of the half-space. The ensuing rigid-body translation and rotation of the strip are determined exactly during the time interval for a compressional wave to traverse the length of the strip. However, the response of the strip, thereafter, appears to be predicted accurately by the solution, based on results for a specific numerical example.

1. INTRODUCTION

STUDIES of elastic wave scattering by obstacles embedded in a half-space are of interest in seismology, in the design of buried structures, and in the general area of dynamic stress concentration about inclusions or cavities located near a boundary of a material. However, such problems have been treated much less successfully than those involving obstacles in an unbounded solid. The presence of the half-space boundary so complicates the scattered wave motion, that analytical descriptions are usually impossible to obtain.

For the case of a rigid plate mounted on top of a half-space, some results are available. Fredricks [1], Fredricks and Knopoff [2] and Gregory [3] have found solutions for scattering of elastic waves by a semi-infinite, rigid-smooth overlay on the surface. Flitman [4] has determined the motion of a finite, rigid-smooth plate mounted on a half-space and subjected to impinging stress waves. His results are exact during the first time interval for a compressional wave to traverse the length of the plate. Also, there is the related work of Karasudhi *et al.* [5] on the radiation of waves in a half-space from a finite plate, vibrating on the surface.

For a buried obstacle, there are a few studies on the radiation of stress waves from a cylindrical and spherical cavity in a half-space [6–9]. However, the iteration solutions obtained so far appear to be accurate only for deeply buried cavities.

This paper presents a two-dimensional study of elastic wave scattering by a rigid-smooth strip embedded directly below and perpendicular to the boundary of a half-space (Fig. 1). The half-space is subjected to a moving pressure wave, because such a loading represents approximately an air blast wave produced by explosions, and also because it generates planar compressional and shear waves incident upon the strip. These are easier to study than the complicated non-planar waves produced by a stationary line load. Exact results are obtained for the rigid-body response of the strip during the first time interval for a compressional wave to traverse its length. The analytical method used is related to that

† This work was supported by Bell Telephone Laboratories, Whippany, N.J.

‡ Associate Professor of Mechanics.

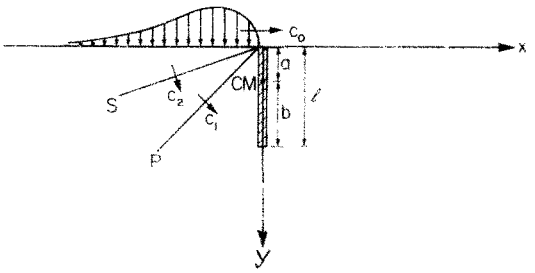

FIG. 1. Geometry and loading for problem.

employed by Flitman [4] and Kostrov [10], the latter of whom treated the scattering of elastic waves by a finite strip in an unbounded medium.

The problem is first divided into diffraction and radiation portions according to the procedure set forth in Ref. [11]. Then short-time solutions in each portion are constructed from exact solutions of two semi-infinite strip problems, viz. the semi-infinite strip dividing a half-space into two quarter-spaces and the semi-infinite strip in an unbounded medium. This approach is valid because the scattering of the waves at each edge of the strip occurs independently until the scattered waves reach the opposite edges. For the diffraction problems, both semi-infinite strip solutions are known [12, 13]. These are briefly reviewed here and the two new radiation solutions are derived. The results are combined to form the equations of motion for the strip.

The paper concludes with an example of a normally incident compressional wave with a rectangular pulse profile. Numerical results are shown for the transition and rotation of the strip and these appear to be accurate beyond the initial time interval in which they are exact. The peak responses occur, however, within the initial time period.

2. DESCRIPTION OF PROBLEM

The geometry for the problem (Fig. 1) consists of an isotropic, elastic half-space ($y > 0$) in which a thin, rigid strip of length l is embedded. The strip has smooth sides and its mass center is located at distances a and b from its top and bottom edges, respectively. A state of plane strain is assumed.

The loading consists of a pressure wave travelling along the surface of the half-space with the constant superseismic velocity, c_0. This wave originated at $x = -\infty$ and it arrives at the top edge of the strip at $t = 0$. It generates in the half-space the steady, planar compressional (P) and planar shear (S) waves which propagate at the speeds c_1 and c_2, respectively. In terms of the shear modulus μ, density ρ and Poisson's ratio ν, of the half-space,

$$c_1 = \kappa c_2, \quad c_2 = (\mu/\rho)^{\frac{1}{2}}, \quad \kappa = [(2-2\nu)/(1-2\nu)]^{\frac{1}{2}} \tag{1}$$

and we assume $c_0 \geq c_1$. Of course for real materials, $c_1 > c_2$.

When the incident P and S waves strike the initially undisturbed strip, they are scattered. Similarly the transient waves, generated to the right of the strip as the pressure wave propagates past it, will be scattered. The problem is to compute the resultant wave fields in the half-space. In particular we calculate the reactions on the strip, from which its rigid-body response is evaluated according to Newton's law of motion.

Boundary conditions along the surface of the half-space specify an arbitrary pressure wave,

$$\tau_{yy}(x, 0, t) = -p(t - x/c_0), \quad \tau_{xy}(x, 0, t) = 0 \tag{2}$$

where $p = 0$ when its argument is negative. Conditions at the smooth sides of the strip specify that the surrounding medium remains in contact, i.e.

$$\left.\begin{aligned} u_x(0, y, t) &= U(t) + (y-a)\Omega(t) \\ \tau_{xy}(0, y, t) &= 0 \end{aligned}\right\} \quad 0 < y < l \tag{3}$$

where $U(t)$ and $\Omega(t)$ are, respectively, the resultant rigid-body displacement in the x-direction and rotation in the counter-clockwise sense about the mass center of the strip. These are calculated from

$$\begin{aligned} m\ddot{U}(t) &= \int_0^l [\tau_{xx}(0^+, y, t) - \tau_{xx}(0^-, y, t)]\,dy \\ I\ddot{\Omega}(t) &= \int_0^l [\tau_{xx}(0^+, y, t) - \tau_{xx}(0^-, y, t)](y-a)\,dy \end{aligned} \tag{4}$$

in which m is the mass of a unit length of the strip normal to the plane of Fig. 1 and I is the moment of inertia about the mass center of such a unit length of the strip. The right-hand sides of equations (4) represent the total force and moment on the strip.

In addition to the above boundary conditions, in order to guarantee a unique solution, we append the "edge conditions" that the displacements are finite at each edge of the strip, $y = 0, l$, and the "radiation condition" that the scattered waves propagate away from the strip.

To represent the P and S waves mathematically we use the wave potentials $\phi(x, y, t)$ and $\psi(x, y, t)$ respectively. These satisfy the equations of motion,

$$(c_1^2\nabla^2 - \partial^2/\partial t^2)\phi = 0, \qquad (c_2^2\nabla^2 - \partial^2/\partial t^2)\psi = 0 \tag{5}$$

and are related to the displacements according to

$$\mathbf{u} = \nabla\phi + \nabla \times \psi\boldsymbol{\varepsilon}_z \tag{6}$$

where $\boldsymbol{\varepsilon}_z$ is a unit vector in the z-direction. The stresses are determined from Hooke's Law as,

$$\tau_{ij} = \mu[u_{i,j} + u_{j,i} + 2\nu\delta_{ij}u_{k,k}/(1-2\nu)] \tag{7}$$

where Cartesian tensor notation is used in (7) with δ_{ij} being the Kronecker delta.

3. SEPARATION INTO DIFFRACTION AND RADIATION PROBLEMS

Mathematically, the problem is to determine the outgoing wave solutions of equations (5) subject to the boundary conditions (2) and (3) and the edge conditions. The solution will depend on the functions, $U(t)$ and $\Omega(t)$ which are then determined explicitly from equations (4). A convenient scheme for accomplishing the analysis was formulated in [11] (and also was used in [4] and [10]). It splits the scattered waves into waves *diffracted* by the strip assumed to be immobile, and a second field of waves *radiated* into the half-space by the

strip moving as a rigid body with amplitudes $U(t)$ and $\Omega(t)$. Thus, in our problem, with incident and scattered waves denoted with superscripts (i) and (s), respectively, the scattered waves are split as

$$\mathbf{u}^{(s)} = \mathbf{u}^{(d)} + \mathbf{u}^{(r)}, \qquad \tau_{ij}^{(s)} = \tau_{ij}^{(d)} + \tau_{ij}^{(r)}. \tag{8}$$

The diffracted waves (d) satisfy the boundary conditions,

$$\begin{aligned} u_x^{(i)} + u_x^{(d)} &= 0 \\ \tau_{xy}^{(i)} + \tau_{xy}^{(d)} &= 0 \end{aligned} \qquad \text{on } x = 0, \quad 0 < y < l \tag{9}$$

indicating a rigid-smooth, immobile strip. The radiated waves (r) then must satisfy,

$$\begin{aligned} u_x^{(r)} &= U(t) + (y-a)\Omega(t) \\ \tau_{xy}^{(r)} &= 0 \end{aligned} \qquad \text{on } x = 0, \quad 0 < y < l \tag{10}$$

where U and Ω are arbitrary functions at this stage. The equations of motion which yield the actual values of U and Ω are derived upon substituting in equations (4) the total force and moment on the strip in each of the separate problems for $\mathbf{u}^{(d)}$ and $\mathbf{u}^{(r)}$. The boundary conditions along the surface of the half-space require that the tractions of the diffracted and radiated fields vanish since the incident waves themselves are excited by the loading (2), i.e.

$$\begin{aligned} \tau_{yy}^{(i)} &= -p(t - x/c_0), \quad \tau_{yy}^{(d)} = \tau_{yy}^{(r)} = 0 \\ \tau_{xy}^{(i)} &= \tau_{xy}^{(d)} = \tau_{xy}^{(r)} = 0 \end{aligned} \qquad \text{on } y = 0 \tag{11}$$

4. THE DIFFRACTION PROBLEM (I)

In the diffraction portion of the problem (I) we calculate the waves scattered by the rigid-smooth strip assumed to be stationary. The incident waves on the left side of the strip are described in Ref. [13] as

$$\mu\ddot{\phi}^{(i)} = -c_0^2(\beta^2 - 1)Np[t - (x + \alpha y)/c_0] \tag{12a}$$

$$\mu\ddot{\psi}^{(i)} = 2c_0^2\alpha Np[t - (x + \beta y)/c_0] \tag{12b}$$

where

$$\begin{aligned} \alpha^2 &= c_0^2/c_1^2 - 1, \quad \beta^2 = c_0^2/c_2^2 - 1 \\ N &= [(\beta^2 - 1)^2 + 4\alpha\beta]^{-1} \end{aligned} \tag{13}$$

and each dot over the wave potentials, indicates differentiation with respect to time. On the right side of the strip, the transient incident waves are rather complicated and it is easier to treat the total field there. This is done subsequently. At this point we present the method for constructing the exact solution for the diffraction problem during the first time interval for a P wave to traverse the length of the strip, i.e. during $0 < t < l/c_1$.

1. *Separation into two semi-infinite strip problems*

Referring to Fig. 1 and the incident waves (12), we find that the incident P and S waves reach the bottom edge of the strip at $t = t_1$ and $t = t_2$, respectively, where

$$t_1 = \alpha l/c_0 \geq 0 \quad (t_1 = 0 \text{ when } c_1 = c_0)$$

$$t_2 = \beta l/c_0 > 0$$

The first diffracted waves (P waves) generated at the top edge of the strip do not reach the bottom edge until $t = \bar{t}\ (= l/c_1)$ and a straightforward calculation shows that $t_1 < \bar{t} < t_2$.

Therefore, for $0 \leq t \leq t_1$ and $x = 0$, no waves have reached the bottom edge of the strip. Consequently the solution is identical to that for an infinitely long strip which divides the half-space into two quarter-spaces [see Fig. 2(a)]. To extend the solution into the interval $t_1 \leq t \leq \bar{t}$, we have to superimpose on the solution of the problem in Fig. 2(a), the solution of the diffraction of the incident P-wave by a semi-infinite strip in an infinite solid [Fig. 2(b)]. Note that the waves diffracted at the bottom edge do not propagate to the half-space boundary until $t = (t_1 + \bar{t}) \geq \bar{t}$.

2. *Solution for* $0 \leq t \leq t_1$

Consider the problem in Fig. 2(a) of a half-space divided into two quarter-spaces by a stationary, rigid-smooth wall and subjected to the moving pressure load. This problem was solved in Ref. [13] and the total reactions on the wall were calculated. Here we list the pertinent results in our problem with subscript 2a to refer to Fig. 2(a). However, in [13] the

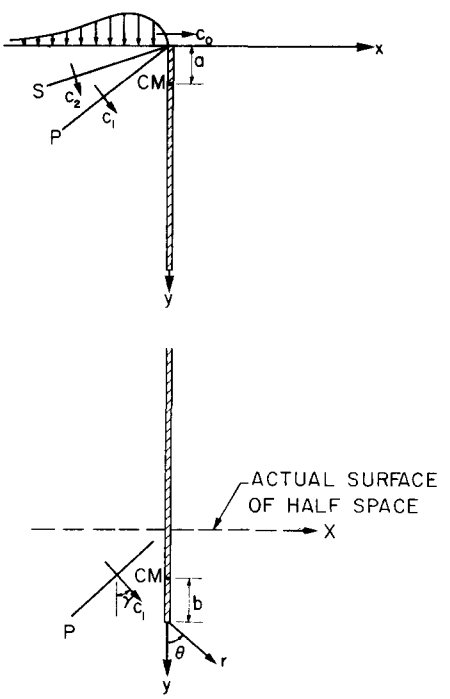

FIG. 2. Models for diffraction portion of problem. (a) Semi-infinite strip in half-space: effects at top edge and sides of strip. (b) Semi-infinite strip in unbounded medium: effects at bottom edge of strip.

wall is assumed to have a finite thickness so that the pressure wave takes t_0 units of time to reach the right-hand quarter-space. Also in [13], the pressure wave has profiles $p_L(t)$ and $p_R(t)$ and velocities c_L and c_R over the left and right-hand quarter-spaces, respectively. Therefore, here we set $t_0 = 0$, $c_L = c_R = c_0$, and $p_L = p_R = p$. Also, we take a counter-clockwise moment to be positive in this paper.

On the left side of the wall are two distinct occurrences. First, the incident P and S waves are reflected as [13],

$$\mu\ddot{\phi}^{(RF)} = -c_0^2(\beta^2-1)Np[t+(x-\alpha y)/c_0] \tag{14a}$$

$$\mu\ddot{\psi}^{(RF)} = -2\alpha c_0^2 Np[t+(x-\beta y)/c_0] \tag{14b}$$

and secondly they are diffracted at the upper corner.† The total reactions on the left side (L) of the wall are obtained from the formulas,

$$F_{2a}^{(L)}(t) = -\int_0^t \tau_{xx}(0^-, y, t)\,dy, \quad M_{2a}^{(L)}(t) = -\int_0^t \tau_{xx}(0^-, y, t)(y-a)\,dy. \tag{15}$$

In our notation, the reactions caused by the incident and reflected waves become,

$$\begin{aligned} F_{2a}^{(i)}+F_{2a}^{(RF)} &= -2c_0\alpha^{-1}N(\beta^2+1)(2\alpha^2-\beta^2+1)[p(t)*1]; \qquad 0<t<t_1 \\ F_{2a}^{(i)}+F_{2a}^{(RF)} &= -2c_0\alpha^{-1}N\Big[(\beta^2+1)(2\alpha^2-\beta^2+1)\int_0^{t_1} p(t-\tau)\,d\tau \\ &\quad +4\alpha^2\int_{t_1}^{t} p(t-\tau)\,d\tau\Big]; \qquad t_1<t<t_2 \end{aligned} \tag{16a}$$

$$\begin{aligned} M_{2a}^{(i)}+M_{2a}^{(RF)} &= 2c_0^2(\alpha\beta)^{-2}[(\beta^2-\alpha^2)(\beta^4-1)N-\alpha^2][p(t)*t] \\ &\quad -a(F_{2a}^{(i)}+F_{2a}^{(RF)}); \qquad 0<t<t_1 \\ M_{2a}^{(i)}+M_{2a}^{(RF)} &= 2c_0^2(\alpha\beta)^{-2}\Big\{[(\beta^2-\alpha^2)(\beta^4-1)N-\alpha^2]\int_0^{t_1}\tau p(t-\tau)\,d\tau \\ &\quad -4\alpha^3\beta N\int_{t_1}^{t}\tau p(t-\tau)\,d\tau\Big\} - a(F_{2a}^{(i)}+F_{2a}^{(RF)}); \qquad t_1<t<t_2 \end{aligned} \tag{16b}$$

and the reactions due to the diffracted waves are

$$F_{2a}^{(D)} = -2c_2^2(\pi c_0)^{-1}\delta_2 I_0[p(t)*1]; \qquad 0<t \tag{17a}$$

$$M_{2a}^{(D)} = [c_0c_2^2(c_0+c_2)^{-1}-2c_2^3(\pi c_0)^{-1}\delta_1 J_0][p(t)*t]-aF_{2a}^{(D)}; \qquad 0<t \tag{17b}$$

where

$$t_1 = \alpha l/c_1, \quad \delta_1 = 1-\kappa^{-2}, \quad \delta_2 = 1-2\kappa^{-2}, \quad \kappa = c_1/c_2,$$

$$I_0 = \int_0^\infty [(\xi^2+\kappa^{-2})^{\frac{1}{2}}(\xi^2+c_2^2/c_0^2)\Omega(\xi)]^{-1}\,d\xi$$

$$J_0 = \int_0^\infty (2\xi^2+1)[(\xi^2+\kappa^{-2})(\xi^2+c_2^2/c_0^2)(\xi^2+1)\Omega(\xi)]^{-1}\,d\xi$$

$$\Omega(\xi) = (2\xi^2+1)^2-4\xi^2[(\xi^2+\kappa^{-2})(\xi^2+1)]^{\frac{1}{2}}$$

† In the left-hand quarter-space, we are splitting further the "diffracted" waves of equations (8) into planar reflected waves (RF) and waves scattered at the corner (D), i.e. $\mathbf{u}^{(d)} = \mathbf{u}^{(RF)} + \mathbf{u}^{(D)}$.

and * denotes the convolution operation,

$$f*g = \int_0^t f(t-\lambda)g(\lambda)\,\mathrm{d}y.$$

The integrals I_0 and J_0 are calculated in [13].

In the right-hand quarter-space it follows from [13] with $t_0 = 0$ and $p_R = p_L$ that the total stress field is identical to the negative of the stress field for the diffracted (D) waves alone in the left-hand quarter-space. Hence, we may write the reactions on the right side (R) of the wall from

$$F_{2a}^{(R)}(t) = \int_0^t \tau_{xx}(0^+, y, t)\,\mathrm{d}y, \quad M_{2a}^{(R)}(t) = \int_0^t \tau_{xx}(0^+, y, t)(y-a)\,\mathrm{d}y \tag{18}$$

as

$$F_{2a}^{(R)}(t) = F_{2a}^{(D)}(t), \quad M_{2a}^{(R)}(t) = M_{2a}^{(D)}(t). \tag{19}$$

The total reactions on the wall in Fig. 2(a) now become

$$F_{2a} = F_{2a}^{(L)} + F_{2a}^{(R)}, \quad M_{2a} = M_{2a}^{(L)} + M_{2a}^{(R)} \tag{20}$$

where

$$F_{2a}^{(L)} = F_{2a}^{(i)} + F_{2a}^{(RF)} + F_{2a}^{(D)}, \quad M_{2a}^{(L)} = M_{2a}^{(i)} + M_{2a}^{(RF)} + M_{2a}^{(D)}$$

To calculate the total reactions in the diffraction problem, we must still consider the scattering of the incident P-wave (12a) by the semi-infinite, rigid-smooth strip shown in Fig. 2(b).

3. *Additional solution for* $t_1 < t < \bar{t}$

In Ref. [12], the problem of Fig. 2(b) is solved exactly for the case of a plane harmonic incident P-wave with the time dependence $\exp(-i\omega t)$. The wave potentials ϕ and ψ are composed of the classical Sommerfeld solutions [14] for diffraction of a plane harmonic wave by a half-plane barrier, plus additional singular terms that are needed to render the displacements finite at the edge. The Sommerfeld solutions occur because the boundary conditions along a rigid-smooth strip, $u_x = \tau_{xy} = 0$, can be expressed equivalently in terms of the potentials as $\partial\varphi/\partial x = \psi = 0$. In other words, the boundary conditions become the same as those in the Sommerfeld problems. However, the potentials are coupled in the edge conditions and this gives rise to the extra singular terms and distinguishes this problem from those of Sommerfeld.

The solution in [12] is in parabolic coordinates and for a configuration that is rotated 90° from that in Fig. 2(b). Therefore, the solution is presented below for our geometry and in the polar coordinates (r, θ) shown in Fig. 2(b). Also, we change $-i\omega$ to s, which is the Laplace transform parameter, and thus obtain the Laplace transform of the solution. The Laplace transform of $f(t)$ is defined as

$$\bar{f}(s) = \int_0^\infty f(t)\,\mathrm{e}^{-st}\,\mathrm{d}t.$$

The justification for this change is that the steady-state harmonic solution in [12] can be interpreted as the Fourier transform of a transient problem with zero initial conditions

and our transient problem in Fig. 2(b) has zero initial conditions.† In this case the two transforms are related through $\omega = is$.

The results are

$$\mu\bar{\phi}(r, \theta, s) = Ar^{-\frac{1}{2}} \sin(\tfrac{1}{2}\theta)\, e^{-s_1 r} + \bar{\phi}_0(s) W_2(r, \theta, \gamma, s_1)$$
$$\mu\bar{\psi}(r, \theta, s) = Ar^{-\frac{1}{2}} \cos(\tfrac{1}{2}\theta)\, e^{-s_2 r} \tag{21}$$

where $s_j = s/c_j$ $(j = 0, 1, 2)$, $\bar{\phi}_0(s)$ is the Laplace transform of the incident wave (12a) at $x = y = 0$,

$$\bar{\phi}_0(s) = -(\beta^2 - 1) N s_0^{-2} \bar{p}(s)\, e^{-s\eta_1} \tag{22}$$

$$A = -2^{\frac{1}{2}}[(s_1\pi)^{\frac{1}{2}}(1+\kappa)]^{-1} \bar{\phi}_0(s) \cos(\tfrac{1}{2}\gamma) \tag{23}$$

$\gamma = \cos^{-1}(\alpha c_1/c_0)$ is the angle of incidence [see Fig. 2(b)] and W_2 is the Sommerfeld solution (with $-i\omega$ replaced by s) for an incident wave of unit magnitude and at angle γ whose normal derivative $(\partial/\partial\theta)$ vanishes on the strip $(\theta = \pm\pi)$. For later reference, we define both W_1 and W_2 where W_1 is the analogous Sommerfeld solution which itself vanishes on $\theta = \pm\pi$.

$$W_{1,2}(r, \theta, \gamma, s_j) = \pi^{-\frac{1}{2}} \left[e^{-s_j r \cos(\gamma - \theta)} \int_{a-}^{\infty} e^{-\lambda^2}\, d\lambda \mp e^{-s_j r \cos(\gamma + \theta)} \int_{a+}^{\infty} e^{-\lambda^2}\, d\lambda \right] \tag{24}$$

with $a \pm = (2s_j r)^{\frac{1}{2}} \sin \tfrac{1}{2}(\theta \pm \gamma)$. Equations (24) and hence (21) contain the sum of the incident and diffracted waves. Note that $\bar{\phi}_0(s)$ in equation (22) contains the "shifting" factor $\exp(-st_1)$ since the initial time for the problem in Fig. 2(b) is $t = t_1$.

Now, we can determine the reactions on the strip in Fig. 2(b). Recall, however, that the incident wave (12a) and the plane reflected wave (14a) have already been considered in the solution of the problem in Fig. 2(a). Therefore, we must subtract the reactions caused by these waves from the reactions due to the solution (21). The details of calculation are lengthy, but straightforward and the Laplace transform of the results is easily inverted. The reactions are calculated from

$$F_{2b}(t) = -\int_0^l [\tau_{\theta\theta}(r, \pi, t) - \tau_{\theta\theta}(r, -\pi, t)]\, dr$$
$$M_{2b}(t) = -\int_0^l [\tau_{\theta\theta}(r, \pi, t) - \tau_{\theta\theta}(r, -\pi, t)](b - r)\, dr \tag{25}$$

where the subscript b refers to the problem in Fig. 2(b), and the net results due to the waves diffracted at the edge alone are

$$F_{2b}(t) = 2c_0^2 c_1^{-1}(\beta^2 - 1) N[2^{\frac{1}{2}}\kappa^2(1+\kappa)^{-1} \cos(\tfrac{1}{2}\gamma) - 2\cos\gamma - \kappa^2(1 + 2^{\frac{1}{2}} \cos(\tfrac{1}{2}\gamma))^{-1}][p(t - t_1) * 1] \tag{26a}$$

$$M_{2b}(t) = 2c_0^2(\beta^2 - 1) N[(2\kappa)^{\frac{1}{2}}(4 - \kappa^{\frac{1}{2}})(1+\kappa)^{-1} \cos(\tfrac{1}{2}\gamma) + \kappa^2(1 + 2^{-\frac{1}{2}} \cos(\tfrac{1}{2}\gamma))(1 + 2^{\frac{1}{2}} \cos(\tfrac{1}{2}\gamma))^{-2} - 2][p(t - t_1) * t] + bF_{2b}(t). \tag{26b}$$

† Zero "initial" conditions in the problem of Fig. 2(b) at $t = t_1$, when the incident wave reaches the bottom edge of the strip, are required so that the combined solution of the problems in Fig. 2 is continuous at $t = t_1$.

The sum of the above reactions with those for Fig. 2(a) [equations (20)] constitute the total reactions on the strip in the diffraction portion of the original problem of Fig. 1 for $0 \leq t \leq \bar{t}$.

$$F_1(t) = F_{2a}(t)+F_{2b}(t), \quad M_1(t) = M_{2a}(t)+M_{2b}(t) \tag{27}$$

5. THE RADIATION PROBLEM (II)

In the radiation portion of the problem the original geometry of Fig. 1 is considered, without any loading and incident waves. The strip is vibrating with amplitudes $U(t)$ and $\Omega(t)$, yielding the boundary conditions

$$\begin{aligned} u_x^{(r)}(0, y, t) &= U(t)+(y-a)\Omega(t) \\ \tau_{xy}^{(r)}(0, y, t) &= 0 \end{aligned} \qquad 0 < y < l \tag{28}$$

Along the boundary of the half-space,

$$\tau_{yy}^{(r)}(x, 0, t) = \tau_{xy}^{(r)}(x, 0, t) = 0. \tag{29}$$

As in the diffraction problem, the solution of the radiation problem can be determined during $0 \leq t \leq \bar{t} = l/c_1$ by a superposition of two semi-infinite, rigid-smooth strip solutions. In the problem in Fig. 3(a), a semi-infinite strip translates and rotates about the point CM according to equations (28) in an infinite medium. The solution, derived below, consists

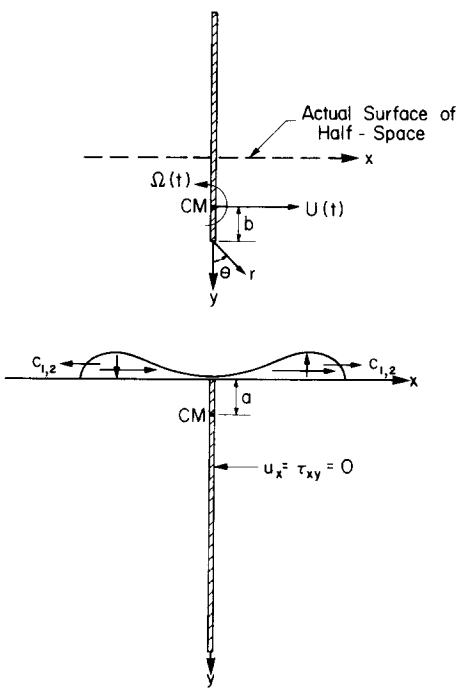

FIG. 3. Models for radiation portion of problem. (a) Semi-infinite strip in unbounded medium: effects at bottom edge and sides of strip. (b) Semi-infinite strip in half-space: effects at top edge of strip.

of plane waves like $U(t-x/c_1)$ which are generated along the sides of the strip and cylindrical waves which emanate from the edge. The latter, however, do not reach the plane $y = 0$ until $t = \bar{t}$. In Fig. 3(b), the half-space is divided into two quarter-spaces by a stationary, rigid-smooth wall and is loaded by the negative of the tractions produced on $y = 0$ by the plane waves radiated in the problem of Fig. 3(a). Therefore, the sum of the solutions for the problems in Fig. 3 is the radiation solution of the original problem for $0 \leq t \leq \bar{t}$.

1. *Radiation solution for Fig.* 3(a)

The boundary conditions along the semi-infinite, rigid-smooth strip in Fig. 3(a) can be written in terms of the wave potentials in the polar coordinates as

$$\begin{aligned} \partial\phi(r, \pm\pi, t)/r\partial\theta &= -V(t)+r\Omega(t) \\ \ddot{\psi}(r, \pm\pi, t) &= 2c_2^2\Omega(t) \end{aligned} \tag{30}$$

where

$$v(t) = U(t)+b\Omega(t). \tag{31}$$

The Laplace transforms of the above equations become

$$\begin{aligned} \partial\bar{\phi}(r, \pm\pi, s)/\partial\theta &= -r\bar{V}(s)+r^2\bar{\Omega}(s) \\ \bar{\psi}(r, \pm\pi, s) &= 2\bar{\Omega}(s)/s_2^2 \end{aligned} \tag{32}$$

where we have again used the zero initial conditions.

Now, the above boundary values (32) along the strip can be produced by introducing the following plane waves (pw) in the field which propagate in the positive x-direction, normal to the strip:

$$\begin{aligned} \bar{\phi}_{pw}(r, \theta, s) &= (-\bar{V}/s_1+\bar{\Omega}\partial/s_1^2\partial\theta)\,\mathrm{e}^{-s_1 r\sin\theta} \\ \bar{\psi}_{pw}(r, \theta, s) &= (2\bar{\Omega}/s_2^2)\,\mathrm{e}^{-s_1 r\sin\theta} \end{aligned} \tag{33}$$

where it is noted that the θ-derivative of a solution of the wave equation is itself a solution. Having introduced these plane waves into the field we must now annihilate them where they actually do not occur (which is everywhere except in $\pi/2 < \theta < \pi$) and yet not alter the boundary conditions. This is done by taking the solution for the diffraction of the negative of the above plane waves by the strip, held immobile, and adding it to equations (33). Thus, consider the incident waves

$$\begin{aligned} \bar{\phi}^{(i)} &= (\bar{V}/s_1-\bar{\Omega}\partial/s_1^2\partial\theta)\,\mathrm{e}^{-s_1 r\sin\theta} \\ \bar{\psi}^{(i)} &= -(2\bar{\Omega}/s_2^2)\,\mathrm{e}^{-s_2 r\sin\theta} \end{aligned} \tag{34}$$

impinging on the semi-infinite, rigid-smooth, stationary strip which now has the boundary conditions

$$\bar{u}_\theta(r, \pm\pi) = \bar{\tau}_{r\theta}(r, \pm\pi) = 0 \tag{35}$$

or equivalently

$$\partial\bar{\phi}/\partial\theta = \bar{\psi} = 0 \quad \text{on } \theta = \pm\pi. \tag{36}$$

According to Section 4, sub-section 3, the solution for diffraction of the waves (34) is expressed in terms of the Sommerfeld solutions $W_{1,2}$ [equations (24)] plus singular, outgoing wave terms. One may check that the results (c) in the entire field are

$$\begin{aligned}\bar{\phi}_c(r,\theta,s) &= Br^{-\frac{1}{2}}\sin(\tfrac{1}{2}\theta)\,e^{-s_1 r} + s_1^{-1}\bar{V}W_2(r,\theta,\pi/2,s_1)\\ &\quad - s_1^{-2}\bar{\Omega}\partial W_1(r,\theta,\pi/2,s_1)/\partial\theta \qquad (37)\\ \bar{\psi}_c(r,\theta,s) &= Br^{-\frac{1}{2}}\cos(\tfrac{1}{2}\theta)\,e^{-s_2 r} - 2s_2^{-2}\bar{\Omega}W_1(r,\theta,\pi/2,s_2).\end{aligned}$$

Note that since $W_1 = 0$ on $\theta = \pm\pi$, so does $\partial^2 W_1/\partial\theta^2 = r^2 s_1^2 W_1 - r^2\partial^2 W_1/\partial r^2 - r\partial W_1/\partial r$ and hence conditions (36) are indeed satisfied by the solution (37). The singular terms in equations (37) are needed to render the displacements finite at the edge of the strip, $r = 0$. It can be shown that the required value of B is

$$B = -[(s_1\pi)^{\frac{1}{2}}(1+\kappa)]^{-1}[2s_1^{-1}\bar{V} - (4\kappa^{\frac{1}{2}} - \kappa^2)s_2^{-2}\bar{\Omega}]. \qquad (38)$$

The complete solution to the radiation problem of Fig. 3(a), indicated with subscripts ($3a$) is given by the sum of equations (33) and (37), i.e.

$$\bar{\phi}_{3a} = \bar{\phi}_{pw} + \bar{\phi}_c; \qquad \bar{\psi}_{3a} = \bar{\psi}_{pw} + \bar{\psi}_c. \qquad (39)$$

Substituting the solution (39) into equations analogous to those in (25), we perform the lengthy, but straightforward, calculation of the Laplace transform of the reactions on the strip and then invert the results to obtain,

$$\begin{aligned}(\mu\kappa^2)^{-1}F_{3a}(t) &= -2lc_1^{-1}\dot{U}(t) - (3-\kappa)(1+\kappa)^{-1}U(t) + l^2c_1^{-1}(1-2bl^{-1})\dot{\Omega}(t)\\ &\quad - (3-\kappa)(1+\kappa)^{-1}b\Omega(t) + c_1[4\kappa^3(1+\kappa)]^{-1}(\kappa^4+9\kappa^3-16\kappa^2+16\kappa+32\\ &\quad - 32\kappa^{\frac{3}{2}})[\Omega(t)*1] \qquad (40a)\\ (\mu\kappa^2)^{-1}M_{3a}(t) &= l^2c_1^{-1}(1-2bl^{-1})\dot{U}(t) - (3-\kappa)(1+\kappa)^{-1}bU(t)\\ &\quad + c_1[4\kappa^2(1+\kappa)]^{-1}(16+16\kappa+5\kappa^2-3\kappa^3-32\kappa^{\frac{1}{2}})[U(t)*1]\\ &\quad - 2l^3c_1^{-1}(3^{-1}-bl^{-1}+b^2l^{-2})\dot{\Omega}(t) - (3-\kappa)(1+\kappa)^{-1}b^2\Omega(t) \qquad (40b)\\ &\quad + c_1b[2\kappa^3(1+\kappa)]^{-1}(16+16\kappa-32\kappa^{\frac{3}{2}}+7\kappa^3-\kappa^4)[\Omega(t)*1]\\ &\quad - c_1^2[4\kappa^4(1+\kappa)]^{-1}(\kappa^5+5\kappa^4-32\kappa^{\frac{5}{2}}+48\kappa-16)[\Omega(t)*t].\end{aligned}$$

To complete the radiation solution, we must determine the reactions on the strip produced in the problem of Fig. 3(b).

2. *Radiation solution for Fig.* 3(b)

As mentioned previously, the solution (39) for the problem of Fig. 3(a) decomposes naturally into plane waves propagating in the positive and negative x-directions and cylindrical waves which radiate from the edge of the strip. The latter do not strike the boundary of the half-space during the time interval of interest. However, the plane waves, which can be shown to be

$$\bar{\phi} = -sg(x)(\bar{T} + y\bar{\Omega})/s_1 e^{-s_1|x|}, \qquad \bar{\psi} = 2\bar{\Omega}/s_2^2 e^{-s_2|x|} \qquad (41)$$

in $x > 0$ and $x < 0$, produce the stresses on the boundary of the half-space, $y = 0$.

$$\begin{aligned} \bar{\tau}_{yy}(x, 0, s) &= -\mu sg(x)(\kappa^2 - 2)s_1 \bar{T} e^{-s_1|x|} \\ \bar{\tau}_{xy}(x, 0, s) &= 2\mu(e^{-s_1|x|} - e^{-s_2|x|})\bar{\Omega} \end{aligned} \tag{42}$$

where $\bar{T} = \bar{U} - a\bar{\Omega}$ and $sg(x) = \pm 1$ for $x > 0$ or $x < 0$, respectively. In deriving equations (41) we used the relations

$$x = r \sin \theta \qquad y - l = r \cos \theta$$

from Fig. 3(a) to express the plane waves (33) in Cartesian coordinates.

The boundary tractions (42) are readily inverted to

$$\begin{aligned} \tau_{yy}(x, 0, t) &= -\mu c_1^{-1}(\kappa^2 - 2)sg(x)\dot{T}(t - |x|/c_1) \\ \tau_{xy}(x, 0, t) &= 2\mu[\Omega(t - |x|/c_1) - \Omega(t - |x|/c_2)]. \end{aligned} \tag{43}$$

Since U and Ω are zero when their arguments are negative it is seen that equations (43) represent moving normal and shear loads over the boundary of the half-space, which originate at $x = t = 0$. To cancel these boundary tractions and yet not alter the conditions along the strip which have been satisfied by the preceding solution, we must add to that solution, the results in the half-space of Fig. 3(b) subjected to the negative of the loading (43). By symmetry, it is seen that we need only consider the right-hand quarter space of Fig. 3(b) as the reactions on the right and left sides of the wall will be equal.

The problem for the right-hand quarter-space of Fig. 3(b) is identified by the boundary conditions,

$$\begin{aligned} \tau_{yy}(x, 0, t) &= \mu c_1^{-1}(\kappa^2 - 2)\dot{T}(t - x/c_1) \\ \tau_{xy}(x, 0, t) &= 2\mu[\Omega(t - x/c_2) - \Omega(t - x/c_1)] \end{aligned} \tag{44}$$

and

$$u_x(0, y, t) = \tau_{xy}(0, y, t) = 0. \tag{45}$$

Now, as explained in [13], the quarter-space problem with a stationary, rigid-smooth vertical boundary can be solved exactly by the method of images. If we consider a half-space subjected to the loading (44) for $x > 0$, and the symmetric image of the normal load and the anti-symmetric image of the shear load for $x < 0$, then conditions (45) along the y-axis are satisfied identically and the solution in this half-space for $x > 0$ is equal to the right-hand quarter-space solution in Fig. 3(b).

We omit the analysis for this half-space problem, which consists of applying the Laplace transform in time and the Fourier transform in x to the governing equations and then obtaining integral representations for the Laplace transform of the solution. Details for solving dynamic half-space problems by this procedure are covered in Fung's text [15]. In our problem, the integral representation for τ_{xx} along the rigid wall, $x = 0$, can be integrated over y to yield the Laplace transforms of the reactions, which are easily inverted. These steps are similar to those used in [13]. The results below have been doubled to

account for the reactions on the left side of the wall in Fig. 3(b).

$$(4\mu\kappa^2)^{-1}F_{3b}(t) = (\kappa^2-2)^2 I_1[U(t)-a\Omega(t)] + c_1\{(\kappa^2-1)(\kappa^2-2)I_2 - [4\kappa^3(\kappa+1)]^{-1}(\kappa-1)(\kappa^3+2\kappa^2-4\kappa-4)\}[U(t)*1] \tag{46a}$$

$$(4\mu\kappa^2)^{-1}M_{3b}(t) = c_1\{(\kappa^2-1)(\kappa^2-2)I_2 - [2\kappa^3(\kappa+1)]^{-1}\}\{[U(t)-a\Omega(t)]*1\} + 4(\kappa^2-1)^2 I_3 c_1^2[\Omega(t)*t] - (4\mu\kappa^2)^{-1}aF_{3b}(t) \tag{46b}$$

where

$$I_1 = \pi^{-1}\int_0^\infty (\xi^2+1)^{-\frac{3}{2}}\Delta(\xi)\,d\xi$$

$$I_2 = \pi^{-1}\int_0^\infty (2\xi^2+\kappa^2)[(\xi^2+1)^2(\xi^2+\kappa^2)]^{-1}\Delta(\xi)\,d\xi$$

$$I_3 = \pi^{-1}\int_0^\infty \xi^2[(\xi^2+1)^2(\xi^2+\kappa^2)^{\frac{3}{2}}]^{-1}\Delta(\xi)\,d\xi$$

$$\Delta(\xi) = \{(2\xi^2+\kappa^2)^2 - 4\xi^2[(\xi^2+1)(\xi^2+\kappa^2)]^{\frac{1}{2}}\}^{-1}. \tag{47}$$

Substitution of $\xi = \tan\theta$ in $I_{1,2}$ and $\xi = \kappa\tan\theta$ in I_3 transforms the above integrals into proper ones which can be evaluated numerically.

The final reactions in the radiation problem are the sum of equations (40) and (46), i.e.

$$F_{II}(t) = F_{3a}(t)+F_{3b}(t); \qquad M_{II}(t) = M_{3a}(t)+M_{3b}(t). \tag{48}$$

Note that the reactions from the radiation solution are independent of the incident wave and so are the same for any loading. In fact, F_{II} and M_{II} are the restoring reactions on the strip due to its "free vibration". Having determined them, we can study the response of the strip for other loadings by calculating only the new input reactions of the diffraction solution.

6. DYNAMIC RESPONSE OF STRIP

The rigid-body response of the strip can now be determined by substitution of the combined reactions, F_I+F_{II} and M_I+M_{II}, in equations (4). Two coupled, integro-differential equations of the convolution type are obtained for U and Ω. However, due to their length in the general case, we illustrate these equations with a specific numerical example. First we introduce the dimensionless time $\tau = c_1 t/l$, dimensionless translation of the strip $u(\tau) = U/l$, and dimensionless pressure wave profile $Q(\tau) = p/\mu$. Also, we define the dimensionless reactions per unit depth of the strip in the z-direction as $F/\mu l\kappa^2$ and $M/\mu l^2\kappa^2$.

In the numerical example, $\nu = \frac{1}{4}$ so that $\kappa^2 = 3$, $a = b = l/2$ which means the mass and geometric centers of the strip coincide, and $c_0 = c_1$ so that the pressure wave generates only a compressional wave in the half-space which is normally incident on the strip, i.e. $\gamma = \pi/2$ in Fig. 2(b). For these choices, $t_1 = 0$ and $\bar{\tau} = c_1\bar{t}/l = 1$. The dimensionless equations of motion, with the reactions (II) written on the left-hand sides then become,

$$\sigma\ddot{u} + 2\dot{u} + 0{\cdot}36u + 0{\cdot}29\Omega - (\Omega*0{\cdot}09) = 2Q + (Q*0{\cdot}36) \tag{49a}$$

$$0{\cdot}29u - (u*0{\cdot}09) + \sigma\ddot{\Omega}/12 + \dot{\Omega}/6 + 0{\cdot}09\Omega + [\Omega*(0{\cdot}16-0{\cdot}05\tau)] = [\Omega*(0{\cdot}29-0{\cdot}09\tau)] \tag{49b}$$

where the decimal fractions are shown here only to two places and the dots now indicate differentiation with respect to τ. The inertia parameter σ is defined as

$$\sigma = \rho_s h/\rho l \tag{50}$$

with ρ_s, h and l being the density, thickness and length of the strip, respectively, while ρ is the density of the half-space medium. Although the analysis until now considered h to be vanishingly small, we must assign, at this point, a finite value to σ in order that the strip have a non-zero inertia. However, h/l should be kept small so that the previous analysis remains meaningful. Here, we choose $h/l = 0{\cdot}05$ and $\sigma = 0{\cdot}24$.

Equations (49), which can be solved by using Laplace transforms, for example, are analogous in part to equations of motion for a coupled, two degree-of-freedom, discrete vibration system. Dashpot and spring force terms occur on the left-hand sides, the former because the radiated energy is absorbed by the surrounding semi-infinite medium and the latter because the medium is elastic. In addition, however, memory-like, convolution force terms appear which are generally absent in discrete networks. They occur in the continuum case because of the waves emanating from the edge of the strip. As these propagate along the strip, they continuously alter its motion, which in turn continuously influences the wave forms of the subsequent waves radiated from the edges. In this way, due to the wave propagation phenomenon, the reactions at time t depend in part on the previous motion.

Although equations (49) are exact for $0 < \tau < 1$, the question arises as to how accurate the solutions become for $\tau > 1$. This question is discussed later, but for now we remark that because of the term $(-\Omega^*0{\cdot}05\tau)$ in equation (49b) the solutions are unstable and become exponentially unbounded as $\tau \to \infty$. Thus, the solutions may be approximately valid for at most a finite period of time beyond $\tau = 1$.

To complete the numerical example, the profile of the pressure wave $Q(\tau)$ is taken as a finite rectangular pulse with unit area,

$$Q(\tau) = \begin{cases} 5 & \text{for } 0 < \tau < 0{\cdot}2 \\ 0 & \text{for } 0{\cdot}2 < \tau \end{cases} \tag{51}$$

whose duration time is less than one. The solutions then become

$$u(\tau) = 5[u_H(\tau) - u_H(\tau - 0{\cdot}2)]; \qquad \Omega(\tau) = 5[\Omega_H(\tau) - \Omega_H(\tau - 0{\cdot}2)] \tag{52}$$

where the responses to the unit step function u_H and Ω_H are given by,

$$\begin{aligned} u_H(\tau) = {} & \tau - 0{\cdot}19e^{-0{\cdot}38\tau} - 0{\cdot}00019e^{0{\cdot}26\tau} + 0{\cdot}06e^{-7{\cdot}4\tau} + 0{\cdot}07e^{-8{\cdot}6\tau} \\ & + e^{-0{\cdot}29\tau}[0{\cdot}06\cos(0{\cdot}87\tau) - 0{\cdot}016\sin(0{\cdot}87\tau)] \end{aligned} \tag{53a}$$

$$\begin{aligned} \Omega_H(\tau) = {} & -0{\cdot}13e^{-0{\cdot}38\tau} - 0{\cdot}004e^{0{\cdot}26\tau} + 0{\cdot}26e^{-7{\cdot}4\tau} - 0{\cdot}19e^{-8{\cdot}6\tau} \\ & + e^{-0{\cdot}29\tau}[0{\cdot}07\cos(0{\cdot}87\tau) + 0{\cdot}20\sin(0{\cdot}87\tau)]. \end{aligned} \tag{53b}$$

Note that the exponentially increasing term in each of equations (53) has a relatively small coefficient so that its contribution is negligible until τ becomes appreciably larger than one.

7. DISCUSSIONS OF NUMERICAL RESULTS AND CONCLUSIONS

The dynamic response of the strip, for the example cited [equations (52)] is presented graphically in Figs. 4 and 5. Figures 4(a–c) show exact results vs. τ in $0 \leq \tau \leq 1$ for the translation of the mass center of the strip, the translation velocity, and the rotation of the strip about its mass center, respectively. The translation increases steadily from $\tau = 0$ to about $\tau = 0{\cdot}6$ where it levels off to a normalized unit value. This is an expected result because the normally incident P-wave (12a) produces the free field x-displacement

$$u_x^{(i)}(\tau) = \begin{cases} 5\tau & \text{for } 0 < \tau < 0{\cdot}2 \\ 1 & \text{for } 0{\cdot}2 < \tau \end{cases} \tag{54}$$

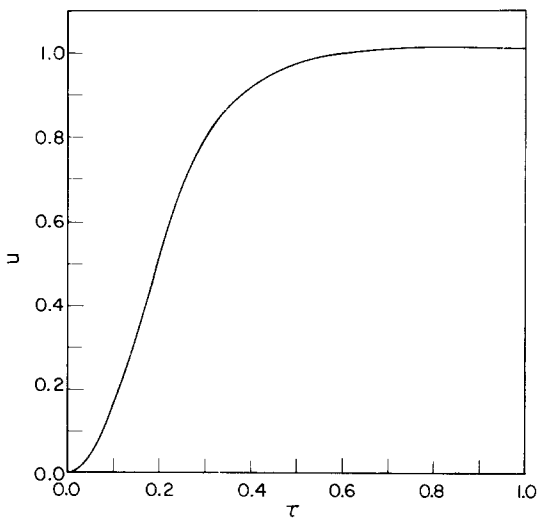

(a)

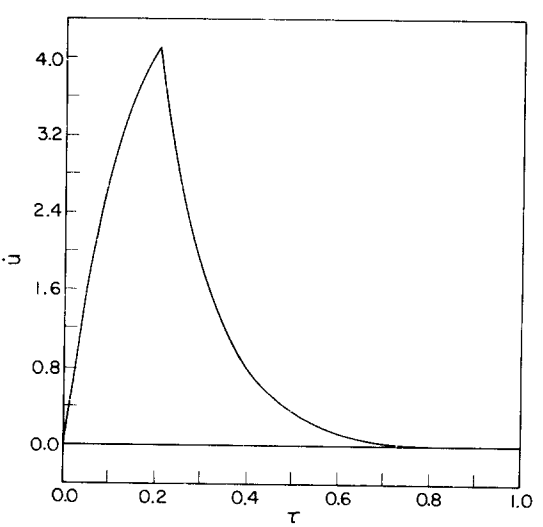

(b)

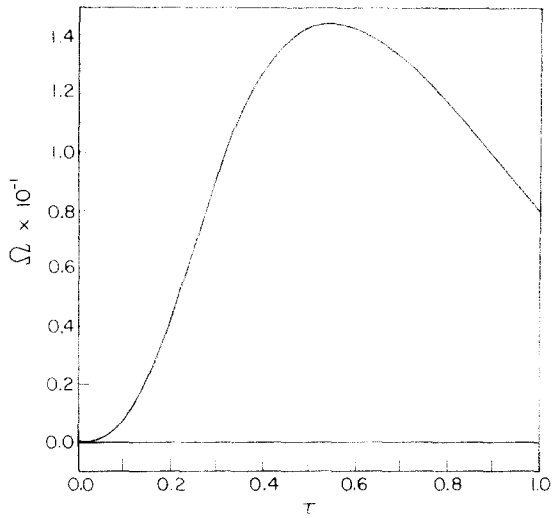

(c)

FIG. 4. Dynamic response of strip vs. dimensionless time $\tau = c_1 t/l$ in $0 \leq \tau \leq 1$. (a) Translation of mass center. (b) Translation velocity of mass center. (c) Angle of rotation about mass center.

which is the unit function with an initial linear rise. Hence, the entire half-space, including the strip is eventually displaced a unit amount in the x-direction. A similar result is reported by Forrestal and Alzheimer [16] for the translation of a rigid cylinder in an unbounded medium due to an incident compressional wave. However, in [16] the incident displacement wave has a ramp function profile and so their curve for the velocity is comparable to our displacement curve, while their acceleration graph is comparable to our velocity results.

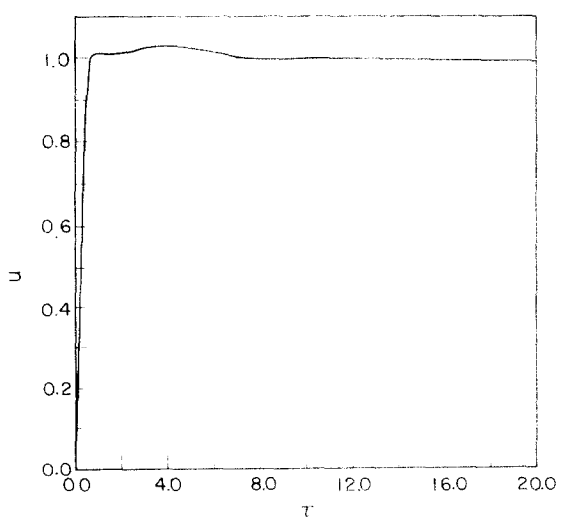

(a)

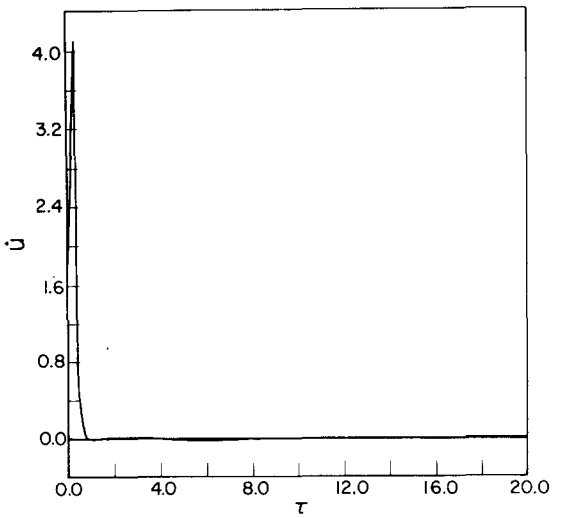

(b)

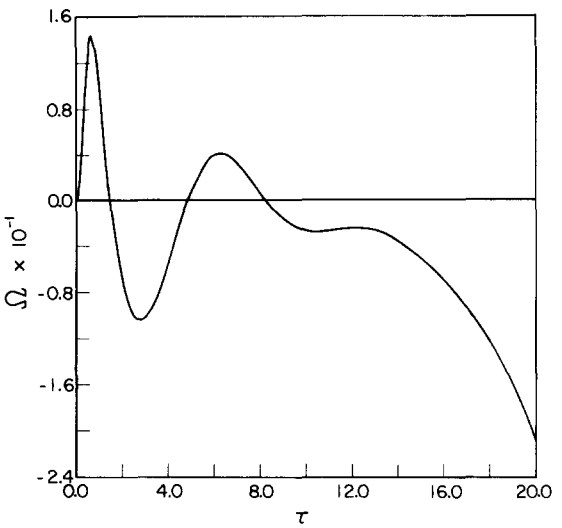

(c)

FIG. 5. Dynamic response of strip vs. dimensionless time τ in $0 \leq \tau \leq 20$. (a) Translation of mass center. (b) Translation velocity of mass center. (c) Angle of rotation about mass center.

The velocity of the strip, in Fig. 4(b), increases steadily until the time when the incident rectangular stress pulse terminates and thereafter, the velocity decreases to zero. Qualitatively, this result compares favorably with the acceleration curves in Ref. [16].

The rotation of the strip, in Fig. 4(c), rises to a peak value of about 0·145 rad. at $\tau = 0{\cdot}55$ and then begins to decrease. Interestingly, for the case of an incident stress wave with a step function profile (not shown here) the rotation reaches its peak value at $\tau = 1$. These results are not directly comparable to any others known to us. For example, in the cylinder

problem of Ref. [16], no rotation occurs. In other plane strain finite strip problems, such as those solved by Kostrov [10] and Flitman [4], no rotation occurs for a normally incident P-wave, because of symmetry.

In order to study the results beyond the unit time period in which they are exact, we present in Figs. 5(a–c) corresponding plots vs. τ for $0 \leq \tau \leq 20$. We observe that the results for the translation and translation velocity remain very close to their expected values of one and zero, respectively, up to $\tau = 20$. In fact, it is not until $\tau = 35$ that the exponentially increasing term in equation (53a) begins to contribute significant figures and causes the results to diverge from their anticipated values. On the other hand, in Fig. 5(c) we see that at about $\tau = 10$, the rotation angle starts to veer from what might be an expected decaying oscillatory curve. This, too, is caused by the exponentially increasing term with negative sign in equation (53b).

In view of the foregoing, it appears that the exact solution derived here for $0 \leq \tau \leq 1$ will remain approximately valid well beyond $\tau = 1$. The results in Figs. 5(a) and 5(b) agree with the physically expected values over the entire time period shown and so it seems reasonable to conclude that the rotation results in Fig. 5(c) are accurate, at least up to about $\tau = 8{\cdot}0$. Physically, it is not surprising that the results should remain valid for $\tau > 1$. What our solution misses are effects of the cylindrical waves generated at the top and bottom edges of the strip after they are rescattered at the opposite edges. Moreover, it is known that such cylindrical waves attenuate at a rate proportional to the inverse square root of their distance of propagation [17]. Hence, we expect their effects will be less significant during subsequent periods of traversal of the strip compared to those during the initial traversal.

Finally, it is noted that our results extend to the physically anticipated "long-time limits". The translation and translation velocity results reach their long-time limiting values even before $\tau = 1$, and the rotation is only about $-0{\cdot}03$ rad. at $\tau = 10$, which is close to the expected limit of zero as $\tau \to \infty$.

Acknowledgements—The author gratefully acknowledges the help of Miss Margaret Wamp and Miss Barbara Cruse of Bell Telephone Laboratories, Whippany, N.J., who performed all numerical calculations.

REFERENCES

[1] R. W. FREDRICKS, Diffraction of an elastic pulse in a loaded half-space. *J. acoust. Soc. Am.* **33**, 17–22 (1961).
[2] R. W. FREDRICKS and L. KNOPOFF, The reflection of Rayleigh waves by a high impedance obstacle on a half-space. *Geophysics* **25**, 1195–1202 (1960).
[3] R. D. GREGORY, The attenuation of a rayleigh wave in a half-space by a surface impedance. *Proc. Camb. Phil. Soc. math. phys. Sci.* **62**, 811–827 (1966).
[4] L. M. FLITMAN, On the motion of a rigid strip mass lying on an elastic half-space and excited by a seismic wave. *PMM* **26**, 1582–1604 (1963).
[5] P. KARASUDHI, L. M. KEER and S. L. LEE, Vibratory motion of a body on an elastic half-plane. *J. appl. Mech.* **35**, 697–705 (1968).
[6] A. BEN-MENAHEM and A. CISTERNAS, The dynamic response of an elastic half-space to an explosion in a spherical cavity. *J. Math. Phys.* **42**, 112–125 (1963).
[7] V. R. THIRUVENKATACHAR and K. VISWANATHAN, Dynamic response of an elastic half-space with cylindrical cavity to time-dependent surface tractions over the boundary of the cavity. *J. Math. Mech.* **14**, 541–571 (1965).
[8] V. R. THIRUVENKATACHAR and K. VISWANATHAN, Dynamic response of an elastic half-space to time-dependent surface tractions over an embedded spherical cavity. *Proc. R. Soc.* **A287**, 549–567 (1965).
[9] V. R. THIRUVANKATACHAR and K. VISWANATHAN, Dynamic response of an elastic half-space to time-dependent surface tractions over an embedded spherical cavity II. *Proc. R. Soc.* **A300**, 159–186 (1967).
[10] B. V. KOSTROV, Motion of a rigid strip-mass soldered into an elastic medium, excited by a plane wave. *PMM* **28**, 113–126 (1964).

[11] S. A. THAU, Radiation and scattering from a rigid inclusion in an elastic medium. *J. appl. Mech.* **34**, 509–511 (1967).
[12] S. A. THAU and Y. H. PAO, Stress intensification near a semi-infinite rigid-smooth strip due to diffraction of elastic waves. *J. appl. Mech.* **34**, 119–126 (1967).
[13] S. A. THAU, Dynamic reactions along a rigid-smooth wall in an elastic half-space with a moving boundary load. *Int. J. Solids Struct.* **4**, 1–13 (1968).
[14] A. SOMMERFELD, Mathematische Theorie der Diffraction. *Math. Ann.* **47**, 317–374 (1896).
[15] Y. C. FUNG, *Foundations of Solid Mechanics*, pp. 218–225. Prentice-Hall (1965).
[16] M. J. FORRESTAL and W. E. ALZHEIMER, Transient motion of a rigid cylinder produced by elastic and acoustic waves. *J. appl. Mech.* **35**, 134–138 (1968).
[17] P. M. MORSE and H. FESHBACH, *Methods of Theoretical Physics*, Part I, p. 842. McGraw-Hill (1953).

(*Received* 30 *December* 1969; *revised* 25 *March* 1970)

Абстракт—Исследуется упругое полупространство, в котором находится тонкая, жестко-гладкая полоса длины l несколько ниже и перпендикулярно к ее поверхности. Полоса подверженная действию плоских, падающих волн сжатия и счвига, которые возникают вследствие постоянно движиющейся волны давления по поверхности полупространства. Определяются в явном виде, трансляция как для жесткого тела и вращение полосы, в интервале времени необходимым для перехода волны давления вдоль длины полосы. Тем не менее оказывается, что воздействие полосы согласно этому является предусмотренное подробно решением, основанным на результатах для специального численного примера.